ELECTROCHEMICAL DETECTION OF ENZYME KINETICS USING A NANOFLUIDIC THIN LAYER CELL DEVICE

E.D. Goluch[1], N. Wongrajit[1], P.S. Singh[1], A.W.J.W. Tepper[2], H.A. Heering[2], G.W. Canters[2] and S.G. Lemay[1,3*]

[1]*Delft University of Technology, THE NETHERLANDS,*
[2]*Leiden University, THE NETHERLANDS and*
[3]*University of Twente, THE NETHERLANDS*

ABSTRACT

Amperometric detection is an attractive detection scheme for mico- and nanofluidic systems as it directly yields an electrical signal. However, this scheme is not often utilized because of its limited sensitivity. We overcome this limitation by employing a nanofluidic device consisting of a solution-filled cavity bounded by two closely spaced parallel electrodes that can amplify the current by repeatedly reducing and oxidizing electroactive species. Here we demonstrate the utility of such a device to measure enzyme kinetics in real time. We compare the conversion of p-cresol into methylquinone by tyrosinase using our nanofluidic device against a standard UV-Vis spectroscopic protocol.

KEYWORDS: Electrochemistry, Redox Cycling, Enzyme Kinetics, Nanofluidics

INTRODUCTION

We have developed a nanofluidic device consisting of two parallel electrodes in a nanometer-scale cavity with openings at either end [1]. Electrochemically active molecules that enter the cavity transfer charge between the electrodes when a potential difference is applied. Typically, electrochemical reactions only involve one or a few electrons per molecule, rendering direct detection of a single molecule in solution virtually impossible. This limitation is overcome, in this situation, by redox cycling, where each molecule can transfer, on average, thousands of electrons by repeatedly traveling between the electrodes before escaping back out into the bulk. In earlier work, we have shown the benefits of such an approach for measuring adsorption [2] and fast electron-transfer kinetics [3]. We have also demonstrated the utility of such an arrangement for sensor applications, where catechol [4] and paracetamol [5] were detected in the presence of excess ascorbic acid.

Here, we present the first experiments using a nanofluidic thin layer cell device in combination with an enzymatic reaction. The reaction kinetics can be monitored directly by the device if the enzyme is capable of converting an electrochemically inactive substrate into an active product as shown in Figure 1. Since the nanochannel is open to the bulk, the composition of the solution inside the device is a representative sample of the bulk solution. Therefore, as the concentration of product in the bulk solution increases, the average number of product molecules in the nanochannel also increases, leading to a larger signal.
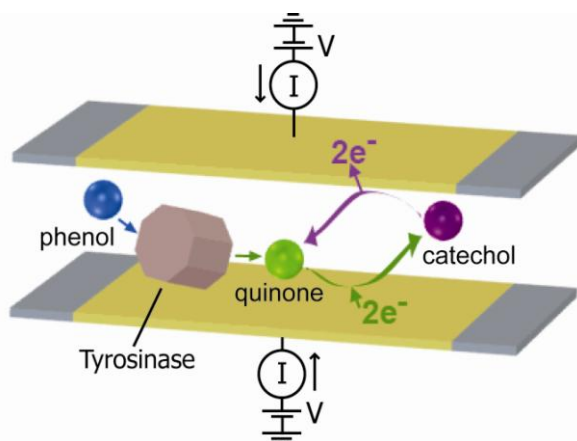

Figure 1: Device concept. Tyrosinase converts inactive phenol molecules into the corresponding active quinones. The quinones are then reduced at the bottom electrode, and after diffusing to the top electrode, are reversibly oxidized. Every cycle, two electrons are shuttled by the molecule from one electrode to the other, giving rise to a steady-state electrochemical current. The current increases as the enzyme creates additional quinone.

EXPERIMENTAL

A micrograph of a completed device is shown in Figure 2. The devices are created using standard microfabrication technology, and can therefore be produced reliably in large quantities. A detailed description of the fabrication process is found in [2]. Briefly, a polished and diced 4-in. silicon wafer with 500 nm of thermally grown SiO_2 was used as the substrate. To create the bottom electrode, first, the wafer was spin-coated with polymethylmethacrylate (PMMA) 950K (4% in anisole) at 5,000 rpm for 60 s, followed by baking at 175 °C for 5 min. The PMMA was exposed in a Leica (EBPG 5000) electron-beam pattern generator using a dose of 1,500 $\mu C/cm^2$ (high tension 100 kV, aperture 400 μm, current 188 nA, BSS 70 nm, spot size 93 nm). The exposed parts were developed using a 1:3 mixture of methylisobutylketone/IPA for 90 s, followed by a 30 s rinse in IPA. After development, the wafer was coated with 4 nm Ti (0.5 Å/s) as an adhesive layer using electron-beam evaporation, followed by 15 nm Au (0.7 Å/s) and 2 nm of Cr (0.3 Å/s) as the top adhesion layer. Metal lift-off was carried out by placing the wafer in boiling acetone with sonication to remove the unexposed PMMA. A new layer of PMMA 950K (9% in anisole) was then spun on the device at 5,000 rpm and baked for 5 min at 175 °C. The PMMA was exposed and developed using the same process as in the previous step, but with a different pattern that defines the structure of the nanochannel. Next, 40 nm of Cr (0.6 Å/s) was deposited and metal lift-off was performed. The remaining Cr, which envelopes the bottom electrode, acts as a sacrificial layer and defines the dimensions of the nanochannel. Next, the top electrode was defined using PMMA 950K (4% in anisole) and electron beam patterning in the same manner as the bot-
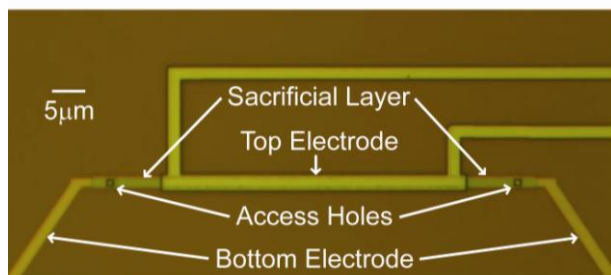
Figure 2: Micrograph of a device (top view). The devices are created using standard microfabrication techniques. Frist, a Au bottom electrode is patterned, followed by a Cr sacrificial layer, a Au top electrode, and an ONO insulation layer. Finally access holes are made and the sacrificial layer is removed via wet chemical etching.

tom electrode and Cr sacrificial layer. The top electrode metal deposition consisted of 2 nm of Cr, 120 nm of Au, and 4 nm of Ti. After metal lift-off, the devices were passivated by sputter deposition of an ONO layer consisting of 300 nm of SiO_2, 200 nm of Si_3N_4, and 100 nm SiO_2. Access holes were defined by patterning PMMA as before. The holes were created using reactive ion etching (Leybold, Cologne, Germany; O_2 2.0 sccm, CHF_3 25 sccm, Ar 16.8 sccm, 150 μbar, 50 W).

Afterwards, individual devices were diced from the wafer. The Cr sacrificial layer was etched away by Cr etchant just prior to using the devices. We have increased the sensor area (75 μm^2) in these devices five-fold versus previously reported results, to increase the current sensitivity of the sensor. Gold electrodes were utilized in the devices as they provide lower background currents than platinum electrodes, allowing lower detection limits.

Purified tyrosinase (monomer, ~30.6 kDa) isolated from *Streptomyces antibioticus* was obtained using the procedure described in [6]. For enzyme immobilization, a procedure similar to that reported in [7] was employed. After removing the Cr sacrificial layer, the devices were rinsed with ethanol and dried thoroughly with a nitrogen stream. The devices were then placed in a 5% v/v solution of 3-glycidoxypropyltrimethoxysilane (GOPS) (Fisher Scientific), a bifunctional linker, to incubate for 30 min with shaking. Next, the devices were rinsed with ethanol, dried with nitrogen for 5 s, and baked at 85 °C for 30 min. The devices were then placed in a 1 μM solution of tyrosinase in 100 mM sodium phosphate buffer for 30 min. The devices were quickly rinsed with deionized water, dried, and used immediately.

Devices both with and without immobilized enzyme were attached to polydimethylsiloxane (PDMS) fluidic reservoirs to allow fluid control. For kinetics experiments, 100 μL of 100 mM sodium phosphate buffer containing 20 nM tyrosinase and varying concentrations of p-cresol was added to the reservoir. A Ag/AgCl (3M NaCl) reference electrode was placed in the solution to measure potentials applied to the electrodes in the device. Two Keithley 6430 remote sourcemeters were employed to apply 0 V to the bottom electrode and 0.300 V to the top electrode while recording the current at both electrodes. For the immobilization experiments, the solution was composed of 100 mM sodium phosphate buffer and 500 μM p-cresol.

RESULTS AND DISCUSSION

We used tyrosinase, an enzyme that converts electrochemically inactive monophenols into active quinones. Figure 3 shows the current response over time for various starting concentrations of *p*-cresol (a monophenol) being converted to methylquinone by the enzyme. We obtained a maximum turnover rate of approximately 1 product/enzyme/second. For comparison, we monitored quinone formation at a wavelength of 400 nm using UV-Vis spectroscopy (Figure 4). The results matched perfectly with our electrochemical detection scheme. By employing electrochemical detection, we are not
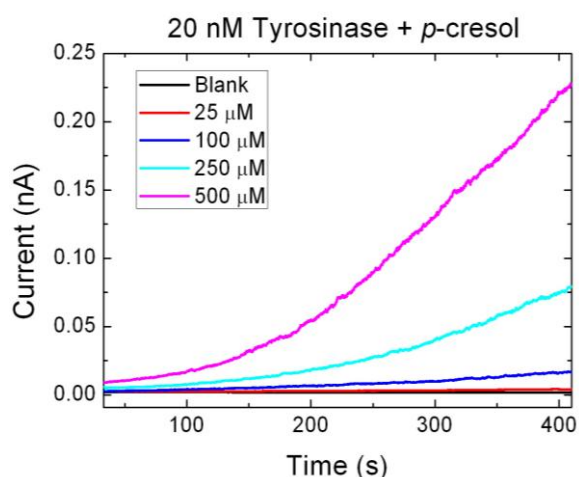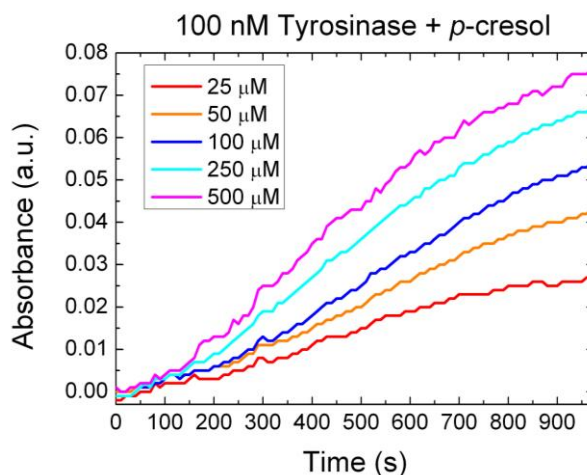

Figure 3: Enzyme kinetics measured using chronoamperometry. The bottom electrode was held at 0 mV and the top at 300 mV relative to a Ag/AgCl (3M NaCl) reference electrode so that redox cycling could take place. 0.10 nA corresponds to 1 μM of product formed. The maximum rate of quinone production matches UV-Vis data.

Figure 4: UV-Vis Data. Quinone concentration measured at 400 nm. Absorption coefficient is 1433M^{-1}cm^{-1}.

limited by the path length of the light as in optical detection and therefore can go to much smaller volumes. In these experiments, 100 µL of solution was used, but further reduction in fluid volume can be implemented.

It is also important for many envisioned experiments to immobilize the enzyme. Figure 5 shows preliminary results with the enzyme immobilized on the device. The immobilization was achieved using a bifunctional linker that attached the enzyme to the exposed oxide surfaces on the device. In this situation, a plateau in the measured current is observed much faster than when the enzyme is freely diffusing, as an equilibrium rate is established between the product molecules reaching the sensor area and diffusing into the bulk fluid reservoir.
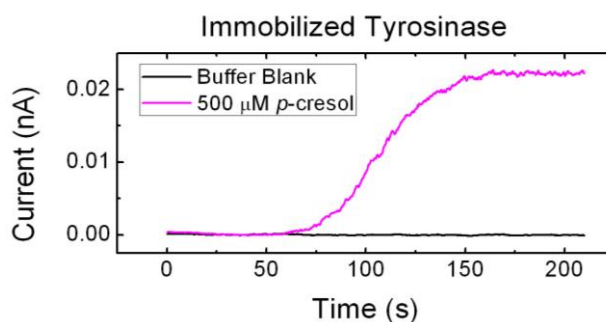

Figure 5: Tyrosinase was immobilized onto the exposed oxide surface of the device. In this case, a plateau in the current was observed as equilibrium was established between the rate at which product molecules enter the sensor area and escape into the bulk fluid reservoir after they are created at the chip surface by the enzyme.

CONCLUSION

We have demonstrated that a nanofluidic device can be employed to monitor enzymatic reactions electrochemically. The kinetic data obtained with our devices matches very well with data acquired using a standard UV-Vis spectrometer, indicating an average turnover rate of 1 product/enzyme/second. Further, we have shown that the enzyme remains active after immobilization and that activity can be measured even with these small amounts of enzyme. This work represents an important first step toward more sensitive enzyme sensors for various applications, ranging from measuring water contamination to electrochemical ELISA detection. Future research will focus on measurement of kinetics from single enzyme molecules and integration with other lab-on-a-chip components.

REFERENCES

[1] M.A.G. Zevenbergen, D. Krapf, M.R. Zuiddam, S.G. Lemay, "Mesoscopic concentration fluctuations in a fluidic nanocavity detected by redox cycling," Nano Letters, **8**, 497 (2007).

[2] M. A. G. Zevenbergen, P.S. Singh, E.D. Goluch, B.L. Wolfrum, S.G. Lemay, "Electrochemical correlation spectroscopy in nanofluidic cavities," Analytical Chemistry, **81**, 8203 (2009).

[3] M. A. G. Zevenbergen, B.L. Wolfrum, E.D. Goluch, P.S. Singh, S.G. Lemay, "Fast electron-transfer kinetics probed in nanofluidic channels," Journal of the American Chemical Society, **394**, 447 (2009).

[4] B.L. Wolfrum, M.A.G. Zevenbergen, S.G. Lemay, "Nanofluidic redox cycling amplification for the selective detection of catechol," Analytical Chemistry, **36**, 3342 (2008).

[5] E.D. Goluch, B.L. Wolfrum, P.S. Singh, M.A.G. Zevenbergen, S.G. Lemay, "Redox cycling in nanofluidic channels using interdigitated electrodes," Analytical and Bioanalytical Chemistry, **22**, 1036 (2009).

[6] A.W.J.W. Tepper, L. Bubacco, G.W. Canters, "Paramagnetic NMR studies of p-nitrophenol binding to tyrosinase," Journal of the American Chemical Society, **127**, 567 (2005).

[7] E.D. Goluch, S.I. Stoeva, J.-S. Lee, K.A. Shaikh, C.A. Mirkin, C. Liu, "A microfluidic detection system based upon a surface immobilized biobarcode assay," Biosensors and Bioelectronics, **24**, 2397 (2009).

CONTACT

*S.G. Lemay, tel: +31-(0)53-4892306; s.g.lemay@utwente.nl